AIMS Energy, 7(1): 77–87.
DOI: 10.3934/energy.2019.1.77
Received: 24 December 2018
Accepted: 28 January 2019
Published: 31 January 2019

http://www.aimspress.com/journal/energy

Review

Shading and masking affect the performance of photovoltaic systems—a review

J. Appelbaum*

School of Electrical Engineering, Tel Aviv University, Israel

* **Correspondence:** Email: appel@eng.tau.ac.il; Tel: +97236409014; Fax: +97236407052.

Abstract: Photovoltaic collectors in the second and in the subsequent rows in a multiple row deployment of PV fields are subject to two effects: Shading and masking both of which reduce the incident solar radiation, and hence reduce the electric energy generated by the PV field. Shading affects the direct beam incident radiation and masking (expressed by the sky view factor) affects the diffuse incident radiation on the PV modules. Both effects depend on field and collector geometric parameters. The result of these effects is uneven distribution of the incident solar radiation on the PV modules, manifested by formation of steps across the I-V characteristic. However, these two effects differ in their nature-shading depends on the movement of the sum and is time dependent whereas masking is position dependent and attains constant values, dependent on geometrical parameters only. Not much attention was paid in the past to the masking phenomenon and its effect on the power loss of PV systems. A series of recent works show that masking in PV fields is an emerging topic of technical significance. Masking may be more detrimental than shading, especially at locations with high percentage of diffuse radiation.

Keywords: PV systems; shading; masking; sky view factor; beam and diffuse radiation

1. Introduction

Photovoltaic (PV) systems are usually deployed in multiple collector rows in PV fields. The rows are separated by a distance. The PV collectors in the second and in the subsequent rows are subject to two effects: Shading and masking both of which reduce the incident solar radiation, and hence, reduce the electric energy generated by the PV field. Shading affects the direct beam incident radiation and masking affects the diffuse incident radiation. Masking is expressed by the view factor

of the collector to the sky (sky view factor). Although both effects are detrimental to the energy generation of the PV field, the energy loss mechanisms are different. Shading depends on the movement of the sun in sky and on field and collector geometric parameters, whereas the sky view factor depends of the geometric parameters only. The shading and masking effects, in this review article, are limited to mutual shading and masking between collector rows. The article does not deal with shading on the PV collectors by overhead wires, poles, trees and other structures, and does not deal with masking on collectors by other obscuring objects.

Figure 1 shows two collector rows facing south. The front (first) collector cast, at a given time, a shadow (gray) of length L_s and height H_s on the second collector. As the shaded and unshaded areas of the collector vary with time during the day, the cells in the PV module are exposed to non-uniform incident solar radiation. Since the cells are connected in series in the PV module, the 'weakest' cell dominates the module performance and therefore, the loss of energy due to shading is un-proportional and is much beyond the shaded area.

While the direct beam radiation is deterministic in nature, the diffuse incident radiation can be envisioned as arriving from multiple sources distributed across the sky-dome. As the sky view factor parameters are associated with different parts on the collector surface, these parts 'see' uneven portions of the sky and consequently, receive different amounts of diffuse radiation (hence receive different amounts of global radiation). In this case, cells on the upper part of the PV module are exposed to higher incident diffuse radiation than cells in other parts, therefore the current mismatch between the cells results in power loss. Both shading and masking are field and collector parameter dependent: Collector width H, collector inclination angle β, row-to-row distance D, and are independent of the collector length for L above 15 meters. These two effects, shading and masking, have technical significance implications because the design of PV system is based on module's rated power for all modules in the PV field. Mitigating these effects may be achieved by decreasing the height ($H \times \sin\beta$) and increasing D. However this approach is bounded by the available land area, generated energy and economic considerations. The purpose of the present article is to provide a review on shading and masking in photovoltaic systems and their effect on the loss of energy, designers of PV system must take into account.

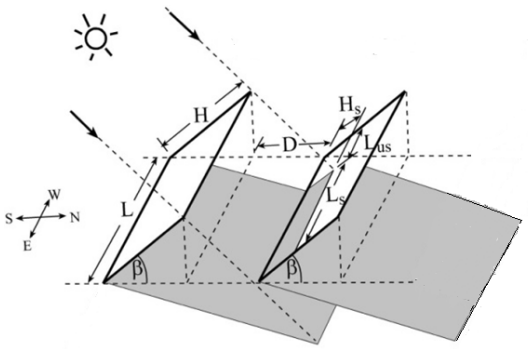

Figure 1. Shading by collectors.

2. Shading

The effect of shading, of various kinds, cast on PV collectors and affecting the I-V characteristics and the performance of the PV systems has been dealt in many articles and will not be mentioned in the present review paper. The present article mentions articles that present the shading on PV collectors (mutual shading) in solar fields by analytical expressions [1–11]. Berra et al. developed an analytical-numerical method for shading calculation for concentrating cylindrical-parabolic collectors in multiple rows [1]. Appelbaum et al. [2]; Jones et al. [3]; Budin et al. [4]; Bany et al. [5]; Groumpos at al. [6]; Elsayed [7,8]; Passias et al. [9]; Thakkar et al. [10]; Quaschning et al. [11] formulate shading expressions for flat plate collectors in multiple row deployments. Bany et al. [5] is an extension study to Appelbaum et al. [2] and the approaches of Jones [3]; Budin et al. [4]; Groumpos et al. [6] are generally similar to Appelbaum et al. [2]; Bany et al. [5], and Elsayed [7]; Elsayed et al. [8] calculate also the shading losses. Passias et al. [9]; Thakkar et al. [10]; Quaschning et al. [11] deal with shading losses of flat plate PV collectors in solar fields.

The shadow height H_s and length L_s is given by [5], respectively:

$$H_s = H(1 - \frac{D + H\cos\beta}{\mathrm{H}\cos\beta + H\sin\beta\cos\gamma_s / \tan\alpha}) \tag{1}$$

$$L_s = L - (D + H\cos\beta)\frac{\sin\beta\left|\sin\gamma_s\right| / \tan\alpha}{\cos\beta + \sin\beta\cos\gamma_s / \tan\alpha} \tag{2}$$

where α is the sun altitude and γ_s is the sun azimuth.

For $\gamma_s > 0$, the shadow is eastward, and for $\gamma_s < 0$, the shadow is westward.

The relative shaded area is:

$$s = \frac{H_s}{H} \times \frac{L_s}{L} = h_s \times l_s \tag{3}$$

where h_s and l_s are the relative shadow height and length, respectively.

Therefore, the direct beam incident radiation G_b^s, in Watts, on a shaded collector becomes [2]:

$$G_b^s = H \times L \times (1 - s) \times G_b \cos\theta \tag{4}$$

where G_b is the direct beam radiation on the collector perpendicular to the solar rays; θ is the angle between the solar ray and the normal to the collector surface.

The amount of shading depends, among others, on the distance D between the collector rows and is usually determined by the shadow length on the ground when the solar elevation angle is at minimum, namely on Dec. 21 at solar noon [12]:

$$D(H,\beta)=\frac{H\sin\beta}{\tan[\sin^{-1}(\cos(\phi-\delta_0))]} \tag{5}$$

where ϕ is the site's latitude and $\delta_0=-23.45°$ is earth's declination angle during winter solstice. Another approach is providing a sufficient distance between the rows for maintenance purposes of the PV system. In optimized PV fields for maximum annual incident energy of the PV field, the distance is determined by the optimization process. An optimized PV field at Tel Aviv, latitude 32^oN, with $H=1.882\,m$, field dimensions $100\times100\,m^2$ resulted in $\beta=17^o$, 38 collector rows and $D=0.85$ m. The difference in direct beam incident radiation between the first (unshaded) and second collector (shaded) is 0.49%. Increasing the distance to $1.5\times D=1.275\,m$ decreases the shading to 0.32%. Applying Eq 5 for $\beta=17^o$, the distance becomes $D=0.8\,m$. For different objective functions of the optimized PV fields, one may obtain different row- to row distances. The difference in the direct bean incident radiation between the first and the second collector is more pronounced with the increase of the inclination angles.

An example of the shadow variation ($h_s=f(l_s)$) on the second collector row of a certain PV field is shown in Figure 2, for morning hours (symmetrical for afternoon hours) on January 21st for two row distances D. The relative shaded area ($h_s\times l_s$) is indicated at 10:00 am. The area for $D=2.07\,m$ is much smaller than for $D=0.8\,m$ and becomes zero from 10:36 am and on, whereas shadow persists all day long for $D=0.8\,m$.

An example of the daily direct beam incident radiation, in kWh, on a second collector row of a PV field on December 21st is shown in Table 1 for an inclined collector row with an angle equal to the latitude $\beta=\phi=32^oN$ and row-to-row distance $D=0.8\,m$. The collector consists 50 modules, $1.293m\times0.33m$ each, arranged in 5 rows; 10 modules in each row. One may notice that the PV modules receive uneven direct beam radiation due to shading, and higher rows (#1 and #2) receive more incident radiation then lower rows (#3, #4 and #5) because higher rows are exposed to direct solar rays for longer time. Row #5 is almost shaded during the day. In summer months the distribution of the direct beam incident radiation on the PV modules is less dispersed.

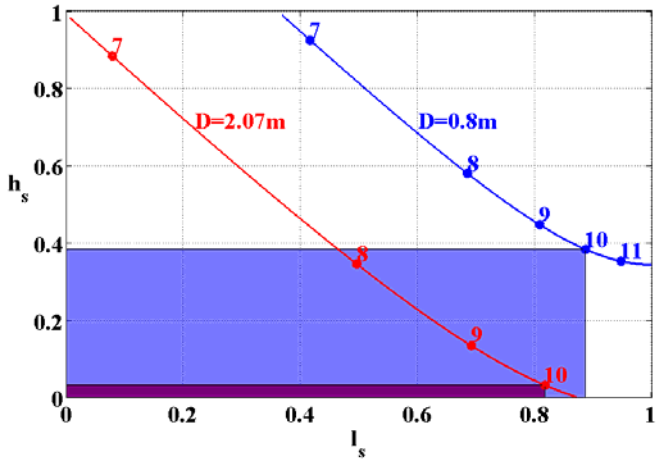

Figure 2. Shadow variation $h_s = \mathrm{f}(l_s)$ for January 21st.

Table 1. Daily direct beam incident irradiation on modules, in kWh, on December 21st.

Row #1	1.19	1.19	1.19	1.19	1.19	1.19	1.19	1.19	1.19	1.20
#2	1.18	1.18	1.18	1.18	1.18	1.18	1.18	1.19	1.19	1.20
#3	1.12	1.12	1.12	1.12	1.12	1.12	1.12	1.12	1.13	1.19
#4	0.53	0.53	0.52	0.52	0.52	0.52	0.53	0.53	0.54	0.69
#5	0	0	0	0	0	0	0	0.01	0.01	0.16

3. Masking

Masking (obscuring part of the sky) of a collector row by a neighboring row is expressed by the sky view factor and is a numerical value formulated by the collector width H, inclination angle β and the distance between the collector rows D, see Figure 1. The sky view factor varies with the distance x along the collector width H, (see Figure 3). The diffuse radiation collected by PV collector is coupled with a view-factor of the collector to sky and may constitute a large portion of the global radiation. The diffuse incident radiation on a PV collector is given by [12]:

$$G_d = F \cdot G_{dh} \tag{6}$$

where G_{dh} is the diffuse radiation on a horizontal plane and F is the sky view factor of the collector.

The daily diffuse radiation is given by [12]:

$$Q_d = A_C \cdot F \int_{\omega_{sr}}^{\omega_{ss}} G_{dh}(\omega) d\omega \tag{7}$$

where A_C is the collector area, Q_d is the daily diffuse energy, ω is the solar hour angle, and

ω_{sr}, ω_{ss} are the sunrise and sunset hour angles, respectively.

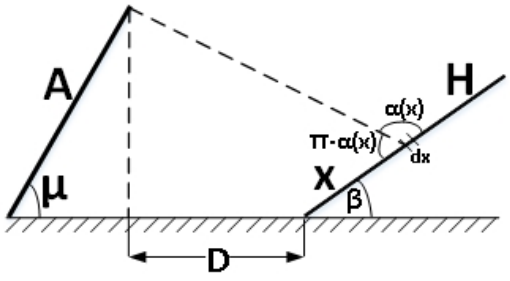

Figure 3. Calculation of the sky view factor.

According to Bany et al.[5] the *local* sky view factor is given by:

$$F_{\alpha(x)} = \cos^2\left(\frac{\pi - \alpha(x)}{2}\right) = \frac{1 + \cos(\pi - \alpha(x))}{2} \tag{8}$$

And the average sky view factor of the entire collector H is therefore:

$$\overline{F_{H\to sky}} = \frac{1}{2H}\int_0^H [1 + \cos(\pi - \alpha(x)]dx \tag{9}$$

For the common case (see Figure 4) where collectors are deployed on a horizontal plane, the sky view factor of the collector H on the right side is [5]:

$$\overline{F_{H\to sky}} = \frac{1}{2} + \frac{\sin\beta}{2}\left\{\cot\beta + d - [(1+d^2]^{1/2}\right\} \tag{10}$$

where $d = D / H\sin\beta$.

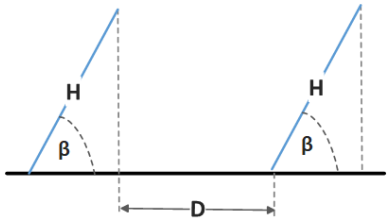

Figure 4. Collectors deployed on horizontal plane.

View factors have wide applications in radiative heat transfer [13–19]. These references deal with thermal radiation between surfaces. In photovoltaic systems, view factors are referred to electric energy generation. Not much attention was paid in the past to the masking phenomenon and its effect on the power loss of PV systems. The detrimental effects of the view factor associated with the

diffuse radiation have been addressed in recent works which established the view factor as an emerging subject of technical significance.

Mathematical expressions for sky view factors for collectors deployed in multiple rows in PV fields are developed in Bany et al. [5]; Maor et al. [20]; Appelbaum et al. [21]. Usually the length of the row is much larger than its width therefore the 'cross-string rule' by Hottel [22] is more convenient to apply than the method in Bany et al. [5]. The view factor between surface S_1 and surface S_2 may be determined with the help of Figure 5.

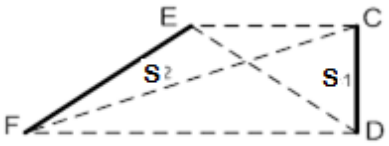

Figure 5. Calculation of view factor between two surfaces.

The view factor is given by:

$$F_{S_1 \to S_2} = \frac{CF + DE - CE - DF}{2 \cdot CD} \tag{11}$$

where CD and EF are the widths of surfaces S_1 and S_2, respectively, ED and CF are the diagonals, and CE and DF are the distances between the surface edges. According to Hottel, the (average) sky view factor of collector H on the right (see Figure 4) is:

$$F_{H \to sky} = \frac{H + D + H\cos\beta - [D^2 + (H\sin\beta)^2]^{1/2}}{2H} \tag{12}$$

And the sky view factor for a single row of collectors, or for the first row in a multiple row field is [23]:

$$F = (1 + \cos\beta)/2 \tag{13}$$

In optimized PV fields, mentioned in Section 2, the view factors of the first, Eq 13 and second collector row, Eq 12 are $F_1 = 0.978$ and $F_2 = 0.934$, respectively. The percentage annual energy loss due to masking (diffuse radiation) on the second collector row caused by the collector in front, amounts to 4.45%. The percentage annual global energy loss due to shading and masking on the second collector row amounts to 1.64%. The incident diffuse radiation on the second and subsequent collector rows dominates the energy loss of the PV field.

Moreover, multiple collector rows of photovoltaic fields containing several modules placed one

above the other along the collector width, experience uneven diffuse incident radiation distribution caused by differences in the modules' sky view factor [12]. For an optimized PV field [12] at Tel Aviv, latitude $32^o N$, with two modules $H = 0.941\,m$ each along the collector width and field dimensions $100 \times 100\,m^2$ resulted in $\beta = 17^o$; 38 collector rows; $D = 0.85\,\text{m}$, the top module collected 6.57% more diffuse energy than the bottom module, because the sky view factor of the top module ($F_1 = 0.966$) is greater than the sky view factor of the bottom module ($F_2 = 0.902$).

The effect of masking is even more detrimental to the PV cells within the module. In typical crystalline silicon PV modules, a common layout is 6 strips of cells (see Figure 6) with 10 cells in each strip. Each strip sees the sky with a different angle, i.e., the local view factor of each strip is different (see Table 2) and consequently, the diffuse incident radiation is different for each strip. As all cells in the module are connected in series, there is a current mismatch between the strips resulting in formation of steps on the I-V characteristic and therefore, reducing the output power of the module [25,26]. The current mismatch is more pronounced in locations where the diffuse radiation consist a large portion of the global radiation. Appelbaum [27] addressed this issue for the first time.

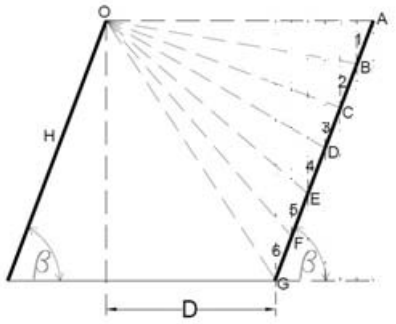

Figure 6. PV module divided by 6 strips.

Table 2. Sky view factors of 6 strips for $\beta = 30°, D = 0.68\,m$ and $H = 0.942\,m$.

$F_1 = 0.9258$	$F_2 = 0.9084$	$F_3 = 0.8850$	$F_4 = 0.8531$	$F_5 = 0.8095$	$F_6 = 0.7507$

Table 2 indicates that the percentage difference in the sky view factor between the top and bottom strips is $\Delta F_{1-6}^{\%} = 100(F_1 - F_6)/F_1 = 18.91\%$. Increasing the inclination angle β causes a reduction of the view factor as the modules in successive rows obscure greater parts of the visible sky. For $\beta = 20°$ the percentage difference is 9.46% and for $\beta = 50°$ it rises up to 39.77% [26]. Peled et al. [26] predicts an overall percentage power loss of the module that ranges 2.8% up to about 25%, depending on the module inclination angle, the row-to-row distance and the

percentage diffuse radiation.

4. Discussion

In multiple collector rows of PV fields the second and subsequent rows are subject to two effects, shading and masking, both of which reduce the electric energy generation of the field. Although both effects are detrimental to the energy generation their energy loss mechanism is different. Shading on collectors depends on the movement of the sun in sky and affects the direct beam incident radiation on the PV modules, and masking affects the diffuse incident radiation on the modules. Both however, depend on field and on collector geometric parameters (H, D, β). Still, as shading depends on the sun movement in sky, the amount of shading and its pattern varies with time during the day along the collector surface. In most times, shading takes place on the ground only and not affecting the collector power output (depending on the row-to-distance). Masking-expressed by the sky view factor- however depends on the geometric parameters only and is constantly independent on time. On the other hand, the value of the view factor is position dependent since it is a local value that varies along the width H of the PV collector. Both effects result in uneven distribution of the incident solar radiation on the PV modules, forming steps across the I-V characteristic and reducing the output power of the modules. Indeed, increasing the row-to-row distance D will reduce shading and masking but will also increase the land area and the length of cables and their costs, increase voltage drops and thus increase the energy loss of the PV field. In some cases, as for rooftops, the available land is limited dictating dense deployments of the PV collectors, thus increasing shading and masking.

5. Conclusions

Shading and masking on PV modules in multiple rows of solar fields lead to current mismatch between the stings of the module, as manifested by the formation of steps on the I-V characteristic, and results in a reduction in the module performance. The effect of shading, of various kinds, cast on PV collectors has been dealt for many years in many articles, however not much attention was paid in the past to the masking phenomenon and its effect on the power loss of PV systems. The detrimental effect associated with masking has been addressed, for the first time, in a series of recent work which established the view-factor as an emerging topic of technical significance. Masking by adjacent collectors in a multiple collector row of PV fields may be more detrimental than shading, especially at locations with high percentage of diffuse radiation, an addressing effect in PV system design.

A distinction should be made between the percentage of shaded area of the module and the percentage of power loss of the module since a PV module contains a series of connected cells including bypass diodes. The percentage of power loss exceeds the percentage of shaded area. The same applies for masking since both effects cause uneven distribution of the incident solar radiation on the modules. The amount of shading and masking depends on parameters of the collector and the PV field (H, D, β); field site; solar radiation data and on objective function of the PV system design. Accordingly, different percentage of power loss may be obtained due to shading and masking. In

optimized PV fields, mentioned in Section 2, the percentage annual global energy loss due to shading and masking on the second collector row amounts to 1.64% (not considering the effect of mismatch currents of the cells in the module). The study in Aronescu et al. [28] reports an energy loss of 5.2% in global energy for $H = 2.0\ m,\ \beta = 30^0, D = 1.0\ m$. Peled et al. [26] predicts an overall percentage power loss of the module that ranges 2.8% up to about 25% (considering mismatch currents within the module). The optimized PV fields, mentioned in Section 2, was carried out at two sites: Tel Aviv, Israel (latitude $32^o N$) with 29% (annual) diffuse radiation and Lindenberg, Germany (latitude $52.2^o N$) with 51% (annual) diffuse radiation. The optimization at Lindenberg resulted in lower inclination angle of the collectors compared to Tel Aviv. This led to reduced shading and masking amounted to 0.47% at Lindenberg compared to 1.64% at Tel Aviv for the annual global energy loss on the second and subsequent rows.

Conflict of interest

The author declare no conflict of interest.

References

1. Barra O, Conti M, Santamata E, et al. (1977) Shadows' effect in a large scale solar power plant. *Sol Energy* 19: 759–762.
2. Appelbaum J, Bany J (1979) Shadow effect of adjacent solar collectors in large scale systems. *Sol Energy* 23: 497–508.
3. Jones Jr RE, Burkhart JF (1981) Shading effect of collector row tilt toward the equator. *Sol Energy* 26: 563–565.
4. Budin R, Budin L (1982) A mathematical model for shading calculations. *Sol Energy* 29: 339–349.
5. Bany J, Appelbaum J (1987) The effect of shading on the design of a field of solar collectors. *Sol Cells* 20: 201–228.
6. Groumpos PP, Kouzam KY (1987) A Generic approach to the shadow effect in large solar power systems. *Sol Cells* 22: 29–46.
7. Elsayed MM (1991) Monthly-averaged daily shading factor for a collector field. *Sol Energy* 47: 287–297.
8. Elsayed M, AI-Turki AM (1991) Calculation of shading factor for a collector field. *Sol Energy* 47: 413–424.
9. Passias D, Kallback B (1984) Shading effects in rows of solar cell. *Sol Cells* 11: 281–291.
10. Thakkar N, Cormode D, Lonij VPA, et al. (2010) A simple non-linear model for the effect of partial shade on PV systems, 2010 35th IEEE Photovoltaic Specialists Conference.
11. Quaschning V, Hanitsch R (1998) Increased energy yield of 50% at flat roof and field installations with optimized module structures, 2nd World Conference and Exhibition on Photovoltaic Solar Energy Conversion, Vienna, Austria, 1993–1996.
12. Appelbaum J, Aronescu A (2018) The effect of sky diffuse radiation on photovoltaic fields.

Renew Sust Energ 10.
13. Mirhosseini M, Saboonchi A (2011) Monte carlo method for calculating local factor for the practical case in material processing. *Int Commun Heat Mass* 38: 1142–1147.
14. Vujicic MR, Lavery NP, Brown SGR (2006) View factor calculation using the Monte Carlo method and numerical sensitivity. *Commun Numer Meth Eng* 22: 197–203.
15. Walker T, Xue SC, Barton GW (2010) Numerical determination of radiative view factors using ray tracing. *J Heat Transfer* 132: 6.
16. Bopche SB, Sridharan A (2009) Determination of view factors by contour integral technique. *Ann Nucl Energy* 36: 1681–1688.
17. Walton GN (2002) Calculation of obstructed view factors by adaptive integration, NISTIR, 6925.
18. Martinez I, Radiative View Factors, 1995–2015.
19. Available from: http://www1.accsnet.ne.jp/~aml00731/c/thermal/View%20factor%20definition.pdf.
20. Maor T, Appelbaum J (2012) View factors of photovoltaic collector systems. *J Sol Energy* 86: 1701–1708.
21. Appelbaum J, Aronescu A (2016) View factors of photovoltaic collectors on roof tops. *J Renew Sust Energ* 8: 1–12.
22. Hottel HC, Sarofin AF (1967), Radiative transfer, McGraw-Hill series in mechanical engineering. New York, 31–39.
23. Duffie JA, Beckman WA (1991) Solar engineering of thermal processes, John Wiley & Sons, Inc.
24. Peled A, Appelbaum J (2016) Minimizing the current mismatch from different locations of solar cells within a PV module by proposing new interconnections. *Sol Energy* 135: 840–847.
25. Peled A, Appelbaum J (2017) Enhancing the power output of PV modules by considering the view factor to sky effect and rearranging the interconnections of solar cells. *Prog Photovoltaic* 25: 810–818.
26. Peled A, Appelbaum J (2018) The view-factor effect shaping of I-V chatacteristics. *Prog Photovoltaic* 26: 273–280.
27. Appelbaum J (2016) Current mismatch in PV panels resulting from different locations of cells in the panel. *Sol Energy* 126: 264–275.
28. Aronescu A, Appelbaum J (2017) Design optimization of photovoltaic solar fields-insight and methodology. *Renew Sust Energ Rev* 76: 882–893.

AIMS Press